THE ANNALS OF "DUNĂREA DE JOS" UNIVERSITY OF GALAȚI
FASCICLE V, TECHNOLOGIES IN MACHINE BUILDING,
ISSN 1221- 4566, 2009

NEWTECH 2009, GALATI

ON THE RESEARCH OF CUTTING COEFFICIENTS IN MACHINING ANNEALED INCONEL 718 WITH CERAMIC TOOLS

David Olvera[1], Gorka Urbicain[1], Norberto López de Lacalle[1]
Daniel Olvera[2], Francisco Javier Campa[1]

[1]University of the Basque Country UPV/EHU, Department of Mechanical Engineering
[2]Monterrey Institute of Technology and Higher Education, ITESM
email: dolvera001@ikasle.ehu.es

ABSTRACT

Nowadays, difficult to cut materials such as nickel and titanium alloys are used more and more frequently because of their excellent behavior even at high temperatures. From this point of view, it is clear the interest of the aeronautical industry in these materials. This paper explores the complex force relationship between the work-piece and the tool during turning of such difficult-to-cut alloys by means of a mechanistic cutting force model which considers the wear force in a new way. The cutting force model demonstrates the sensitivity of the forces to any disturbance of the cutting conditions (a_p, f, V_c) when using ceramic inserts. Obtaining a good accuracy of such coefficients is a key issue to a refined prediction of dynamic stability during machining.

KEYWORDS: Inconel 718, ceramics, cutting coefficients.

1. INTRODUCTION

With the introduction of gas turboreactors, the behaviour of the motor has been developed and ameliorated at every level. The use of new advanced materials has played a major role on this improvement: up to 50% of the increase obtained in turbines' efficiency is attributed to new materials design and manufacture. The development of nickel-based super alloys has lead into an increase in the turbine entrance temperature up to 350˚C over the last decades. During the next 15 years, an increase of 200˚C in the gas turbine entrance temperature is estimated.

Inconel 718, which is a Fe-Ni based super alloy (Ni: 25-60% and Fe: 15-60%) hardened mostly with γ'' phase (Ni_3Nb with BCT scheme), is widely used in the aircraft industry due to its capacity to keep its mechanical properties at high temperatures (700˚C). However, these alloys are also difficult-to-cut materials (high specific cutting force) because of their tendency to work hardening and their high shear strength. The highly abrasive nature of the carbide particles reduces tool life and produces poor surface finish. Because of that, the thermo-mechanical and chemical phenomena between the tool inserts and the machined surface need to be explored.

In order to define appropriate tool geometry and cutting conditions for such difficult to cut materials, previous research work have been carried out under the concept of high speed machining (HSM) and employing carbide tools in the turning process. Fang and Wu [6] explain a detailed comparative machining study between Inconel 718 and Ti-6Al-4V, finding empirical relationships to predict cutting forces depending on cutting speed and feed rate. Thakur et al.[9] studied the wear effect over the tool and showed the trends in the surface finish under different cutting conditions.

On the other hand, the growing trend to increase the productivity and to reduce the coolant consumption during machining, has turned attention to ceramic tools, which deal appropriately with the high temperatures reached during the machining of Fe-Ni based alloys and make dry cutting possible. In this issue, several authors have investigated: Arunachalam et al. [1] analyzed the CBN and mixed ceramic (Al2O3 and TiC) tools behaviour using optimal cutting parameters [2], observing the residual stresses and surface integrity. Narutaki et al. [8] studied the wear resistance of several ceramic tools during severe turning conditions up to 500 m/min.

A more complete state of the art in the field of ceramics and Inconel 718 machining can be observed in the work of Dudzinski et al. [4].

In this study, cutting experiments were carried out in Inconel 718 using ceramic inserts to obtain specific cutting forces. Those basic cutting data are necessary to study the complex relationship between tool and such low machinability material. From them, the effects of the depth of cut and the cutting speed on tool flank wear were also investigated. Future work will focus on modelling system dynamics to forecast cutting conditions in stable zones.

2. FORCE MODELLING

The total force during the cutting process is here divided in 2 main components. Firstly, a cutting force due to the chip removal process, which it is supposed to remain steady along the process. Secondly, a component due to the wear phenomena during the cutting process is considered. This component is time dependent as it is shown in the equation (1) for modelling the total force during the chip removal process.

$$F(t) = F_{cutting} + F_{wear}(t) \qquad (1)$$

At the same time, the cutting force is subdivided into two effects: the force due to the shear stress F_c, which is the dominant component of the process and responsible of the majority of the energy consumption and, secondly, the edge force F_e at the rake surface, due to the friction contact between the chip and the tool insert produced during chip evacuation. If those three effects are separated, the equation results as follows:

$$F(t) = F_c + F_e + F_w(t) \qquad (2)$$

2.1. Shear force

The shear force F_c is responsible of the metal cutting process itself. Using the linear model and introducing the effects of the side cutting edge angle and the depth of cut (a_p) inside the cutting coefficient, the cutting force can be expressed as a function of the feed. It is clear that a cutting coefficient obtained in such way, will have sense only at a specific depth of cut.

$$F_{cx}(a_p) = K_{cx}(a_p) \cdot f \qquad (3)$$

where K_{cx} is the shear cutting coefficient for the x direction, a_p the depth of cut and f the feed per revolution. Similar relationships are found for the y and z directions.

2.2. Edge force

In spite of the studies concerning the tool flank wear effect, the interaction between the work surface and the tool flank is still not well understood. From the works of Kobayashi and Thomsen [7], Thomsen et al. [10] and Zorev [11], it can be said that the deformation located in the primary shear zone and the friction phenomena on the rake face are not affected by the flank wear, that is, the basic cutting quantities remain unaffected by the tool wearland size. Another aspect observed is that flank wear tends to stabilize the system mainly at low spindle speeds: this is the so-called process damping effect.

In this way, the edge force is considered as the friction, adhesion and diffusion phenomena over the chip-rake face can be written as:

$$F_{ex}(a_p) = K_{ex}(a_p) \qquad (4)$$

where K_{ex} is the specific edge force in x direction. Similar relationships are found in y and z directions.

2.3 Wear force

Two main different routes of research have been used to model the effect of the tool flank wear. The first approach based on the contact force model [5, 12] establishes a proportionality relationship between the contact force and the displaced volume of the workpiece beneath the tool. This model is suitable for mild turning but not for hard materials because of the difficulty in estimating the displaced volume. Besides, the measurement of the flank wear length (VB) gets complicated for ceramic inserts, where the cutting is so aggressive. The other proposed approach is based on the slip-line model [3]. In this model, the frictional force, which opposes the sliding of a hard relatively smooth surface over a softer one can be assumed as the force needed to push waves of plastically deformed material along the soft surface ahead of asperities on the hard surface. Kobayashi and Thomsen considered the slip-line field and the plastic flow under the tool flank. Waldorf introduced non-uniform load distribution along the flank wear area to estimate the ploughing force.

In this work, an alternative view of the edge wear is put into practice for the prediction of the total forces. The simplicity of the proposed method lies basically in the fact that it does not include any considerations onto the tool-workpiece material interaction. As the forces involved during machining of low-machinability materials are strongly time dependent, even more if using ceramics tools (because of the high cutting speeds and temperatures reached), it seems reasonable, as a first approach to the wear force analysis, an expression as:

$$F_{wx}(t) = K_{wx}(a_p)\frac{V_c}{V_f}t \qquad (5)$$

where K_{wx} is the specific edge force in x direction as function of the depth of cut. Further on, the

physical sense and composition of this coefficient will be explained. The formula also shows a ploughing force proportional to the chip evacuation velocity given by the cutting speed and an inversely proportional dependence on the feed rate.

3. EXPERIMENTAL SETUP AND DATA ADQUISITION

The cutting experiments were conducted in a CMZ TBI-450MC turning centre with a FAGOR 8050T numeric control, fig. 1. The work-piece, a cylinder of annealed Inconel 718 (Ø100 mm X L300 mm), was clamped using a tailstock and machined at different depths of cut using rhombic ceramic inserts supplied by NTK Cutting Tools with reference CNGN120708T00520 WA1. This is a whisker-reinforced composite ceramic material with silicon-carbide whisker added to alumina, the main component.

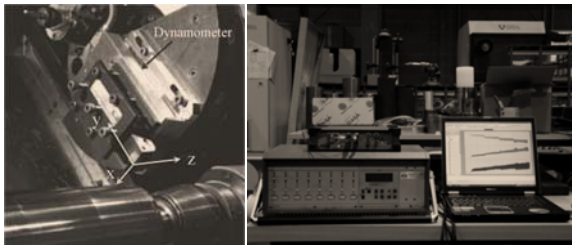

Fig. 1. Experimental setup.

The cutting data recording system used was mainly composed by a KISTLER dynamometer type 9257B and a signal amplifier type 5017, an OROS multichannel analyzer conducted by NV-GATE software 6.2 and a PC for data processing and manipulation.

The cutting tests were performed at two different cutting speeds: V_c = 250 and 300 m/min. Under six different depths of cut: a_p from 0.4 to 0.9 mm, in steps of 0.1 mm. Finally, four different feed rates were tested for each of the depths of cut evaluated, f = 0.05, 0.1, 0.15, 0.2 mm/rev. Each of the series was conducted with a new insert and the wear was measured at the end of the cutting experiment.

4. CUTTING FORCE ANALYSIS

The typical signal of the force measurement during the cutting processes is shown in fig. 2. In order to capture only the effect of the cutting process, and neglecting the wear effect over the tool, the force magnitude was measured in seven points for each experiment. At the beginning of the first feed rate, and in the transition point between two different feed rates.

In this way, the forces due cutting process under each feed rate can be defined as:

$$\begin{aligned} F_{f=0.05} &= F1 \\ F_{f=0.10} &= F_{f=0.05} + \Delta 1 \\ F_{f=0.15} &= F_{f=0.10} + \Delta 2 \\ F_{f=0.05} &= F_{f=0.15} + \Delta 3 \end{aligned} \qquad (6)$$

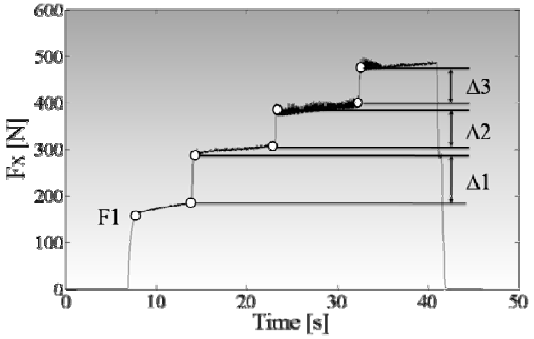

Fig. 2. Example of a single direction signal force measurement using four different feed rates.

Following the criterion described above, the force components due to the cutting process show the behaviour represented in the left side of fig. 3. For the subsequent analysis of the measured forces, a linear regression was carried out at each depth of cut under the four different feed rates adopting the form:

$$F = K_c \cdot f + K_e \qquad (7)$$

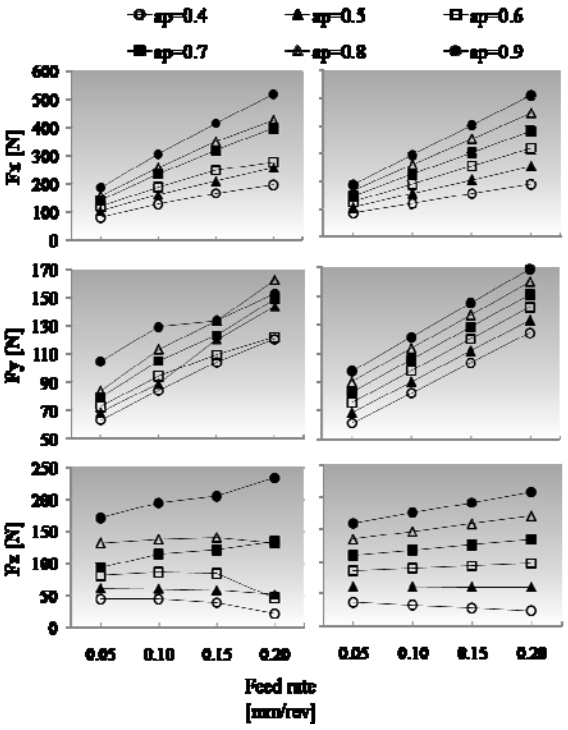

Fig. 3. Experimental cutting forces without the wear effect and linearization for V_c = 250 m/min.

In this way, the slope of each linearization represents the shear cutting coefficient and the y-intercept represents the cutting coefficient due to the edge force. The results of the whole analysis for the cutting coefficients over the two cutting speeds show a linear tendency as the depth of cut increases, fig. 4.

The resulting equations to describe the cutting coefficients are shown in Table 1 and Table 2. From these equations is possible to make a semi-analytical prediction of the forces without consider the wear effect. These predictions shows a good agreement with the experimental data as the fig. 3 illustrates in the graphs located in the right side.

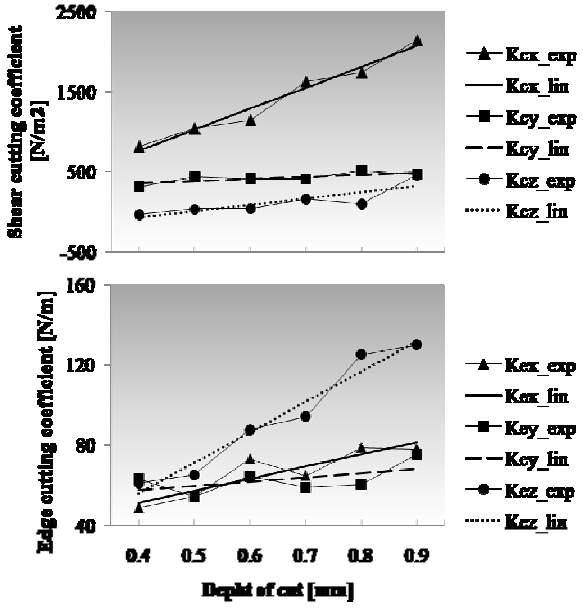

Fig. 4. Experimental linearized cutting coefficients.

An example of prediction for the cutting force, using the expressions described above, is illustrated in the fig. 5. It is evident that the consideration of the increasing wear effect over the force would improve the accuracy between experimental data and predictions. This is a key issue when cutting low-machinability materials with ceramic inserts resulting in an accumulative effect over the forces.

The proposed treatment for the computation of wear effects will be discussed in the next section.

Table 1.Shear cutting coefficient functions. Dependence on the depth of cut.

Shear cutting coefficient
$K_{cx} = 2628.5 \cdot a_p - 296.5$
$K_{cy} = 276.6 \cdot a_p + 241.5$
$K_{cz} = 797.1 \cdot a_p - 391.2$

Table 2. Edge cutting coefficient functions. Dependence on the depth of cut.

Edge cutting coefficient
$K_{ex} = 60.4 \cdot a_p + 26.8$
$K_{ey} = 21.2 \cdot a_p + 48.7$
$K_{ez} = 152.0 \cdot a_p - 5.3$

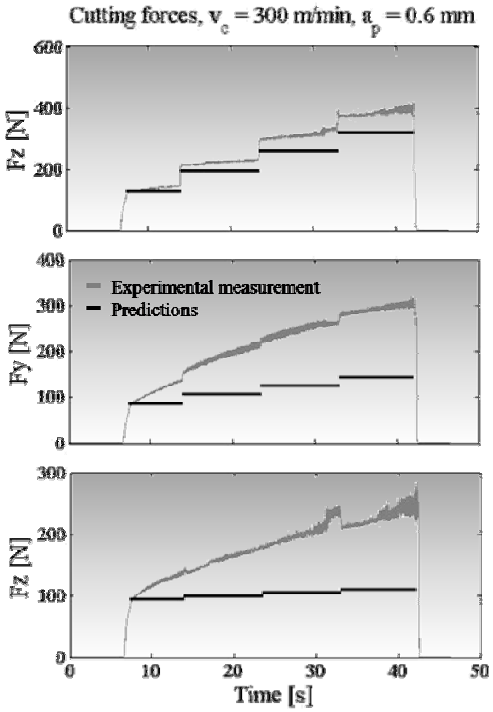

Fig. 5. Force prediction neglecting the wear effect.

5. WEAR FORCE ANALYSIS

From the fig. 4 it can be observed that there is a constant slope between experimental signal and the predicted cutting force. This slope due to the wear effect is constant along each feed rate but slightly varies from one to another. Let K_w the ratio between increasing force and time and Δt_1 the length for the first feed rate. From equation (7), it can be said that the force at the beginning of the first feed rate could be expressed as:

$$F_{1,st} = K_c(a_p) \cdot f + K_e(a_p) \qquad (8)$$

Then, considering the wear increasing effect, the force at the end of the first feed rate is defined by:

$$F_{1,end}(\Delta_{t,1}) = F_{1,st} + K_w \frac{V_c}{V_f} \Delta t_1 \qquad (9)$$

where, K_w is the wear coefficient to determine the effect in the force in N/s. Thus, under the

consideration that there is not significant wear in the transitions between feed rates, the force at the beginning of the second feed rate is:

$$F_{2,st} = F_{1,end} + \Delta 1 \qquad (10)$$

The same procedure can be extended to predict the total force as dependent on time when the wear effect provokes an increasing effect over the cutting forces.

The analysis followed to obtain the wear coefficients for the time dependent term in equation (9) uses again a linear approach, as it was explained for K_c and K_e coefficients. The analysis attempts to find the relationship between the slope force-time as dependent on the depth of cut. The expressions found to describe this wear coefficient are showed in Table 3.

Table 3. The wear coefficient functions depending on depth of cut.

Wear cutting coefficient	
V_c = 250 m/min	Vc = 300 m/min
$K_{wx} = 0.1474 \cdot a_p + 0.4338$	$K_{wx} = 0.1987 \cdot a_p + 0.5845$
$K_{wy} = 0.3850 \cdot a_p + 0.7763$	$K_{wy} = 0.6186 \cdot a_p + 1.2475$
$K_{wz} = 0.6226 \cdot a_p + 0.5504$	$K_{wz} = 0.9714 \cdot a_p + 0.8589$

The force estimated considering the effects of the cutting process as well as the effect introduced by the wear as the tool's life decreases is shown in the Figure 6. It is clearly appreciated a better match between experimental measurements and predictions executed by the force model proposed.

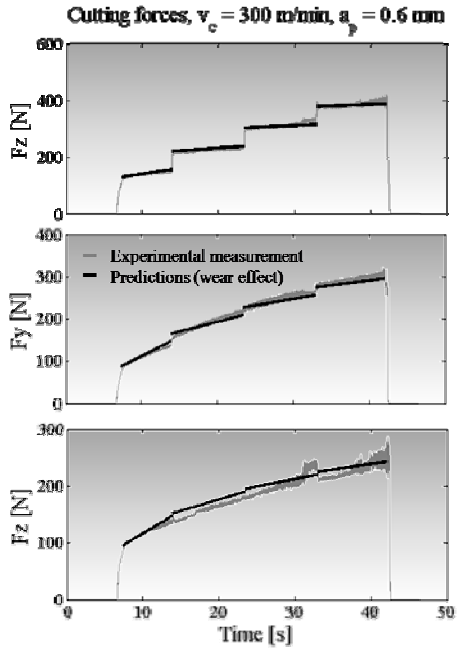

Fig. 6. Force prediction considering the wear effect.

6. CONCLUSIONS AND FUTURE WORK

Knowing the forces or, at least, having a good estimation has been always a subject of matter because of the time-saving in experimental tests. The problem gets more complicated if using the couple Inconel 718-ceramics. This study shows a new way to forecast the forces during the turning process based on a linearization of the wear phenomena. This linearization of the wear processes lies in the slope observed during the experiments in any of the cutting conditions used. Because of the aggressive cutting (high temperatures and stresses due to high cutting speeds), the flank wear effects need to be included in the prediction of the global forces. In fact, the weight of the wear component into the total forces seems to be so variable that a good prediction cannot be achieved without considering the ploughing effects.

This work proposes a different approach for the inclusion of the wear forces in the force model. As it has been explained, the model considers the wear coefficients' deviation with the depth of cut offering a set of equations for different cutting speeds. Similar relationships are found for cutting and edge coefficients. The effects of the feed rate are included for the cutting and wear terms in the general expressions (f for equation (8) and V_f for equation (9)).

Therefore, it is possible, for given cutting conditions (a_p , f , V_c), to predict the forces put into play when the tool has been machining during a certain time t . The model achieved has been adjusted in the width range from V_c = 250 to 300 m/min.

Future work will focus on dynamic description of the system with the inclusion of the wear coefficients into the dynamic stability equation. This relationship must be resolved to obtain the stability lobes, which define vibration free cutting conditions (no chatter). It is well known that process damping phenomena, which are severe distortion sources of these curves at low spindle speeds, are strongly related to the flank wear effects. A system created in such manner should perform the chatter predictions when machining with ceramic inserts is carried out.

ACKNOWLEDGEMENTS

The present research work is framed within the OPENAER project ('Nuevas Configuraciones de Avión y Motor para el Futuro Sistema de Transporte Aéreo'), which belongs to the CENIT program. We are very thankful for the support given by: Industria de Turbopropulsores S. A. (ITP) and Mitsubishi Materials Corporation as materials and tool suppliers respectively.

REFERENCES

[1] Arunachalam, R.-M., Mannam, M.-A., Spowage, A.-C., *Residual stress and surface roughness when facing age hardened Inconel 718 with CBN and ceramic cutting tools*, International Journal of Machine Tools & Manufacture, 44, 2004,pag. 879-887;

[2] Arunachalam, R.-M., Mannan, M.-A., *Performance of CBN cutting tools in facing of age hardened Inconel 718*, Transactions of NAMRI/SME, XXXII, 2004;

[3] Challen, J.-M., Oxley, P.-L.-B., *An explanation of the different regimes of friction and wear using asperity deformation models*, Wear, 53, 1979, pag. 229-243;

[4] Dudzinski, D., Devillez, A., Moufki, A., Larrouquère, D., Zerrouki, V., Vigneau, J., *A review of developments towards dry and high speed machining of Inconel 718 alloy*, International Journal of Machine Tools & Manufacture, 44, 2004, pag. 439-456;

[5] Elbestawi, M.-A., Ismali, F., Du, R.-X., Ullagaddi, B.-C., *Modeling machining dynamics including damping in the tool-workpiece interface*, Tribological Aspects in Manufacturing, 54, 1991, pag. 253-258;

[6] Fang, N., Wu, Q., *A comparative study of the cutting forces in high speed machining of Ti-6Al-4V and Inconel 718 with a round cuting edge tool*, Journal of Materials Processing Technology, 209, 2009, pag. 4386-4389;

[7] Kobayashi, S., Thomsen, E.-G., *The role of friction in metal cutting*, Journal of Engineering for Industry, 82, 1960, pag. 324.

[8] Narutaki, N., Yamane, Y., Hayashi, K., Kitagawa, T., *High speed machining of Inconel 718 with ceramic tools*, Annals of CIRP, 42, 1993, pag. 103-106;

[9] Thakur, D.-G., Ramamoorthy, B., Vijayaraghavan, L., *Study on the machinability characteristics of superalloy Inconel 718 during high speed turning*, Materials and Design, 30, 2009, pag. 1718-1725;

[10] Thomsen, E.-G., Macdonald, A.-G., Kobayashi, S., *Flank friction studies with carbide tools reveal sublayer plastic flow*, Journal of Engineering for Industry, 84, 1962, pag. 53;

[11] Zorev, N.-N., *Metal cutting mechanics*, First Edition. 1966, Oxford: Pergamon Press. Pag. 526;

[12] Wu, D.-W., *Application of a comprehensive dynamic cutting force model to orthogonal wave generating processes*, International Journal of Mechanical Sciences, 30, 1988, pag. 581-660.